RW Materials 2024, 01, 29-38. https://doi.org/10.70498/rwm/20240005 journal homepage: https://www.rwpublisher.com/journal/rw-materials





# Effect of nanoparticle type and processing technique on the performance of lap shear joint of epoxy nanocomposite adhesives

# M.S. Goyat<sup>1,2</sup>

#### **ABSTRACT**

The effect of optimum concentration of TiO<sub>2</sub>, Al<sub>2</sub>O<sub>3</sub> and ZrO<sub>2</sub> nanoparticles on lap shear joint strength and joint toughness (area under the engineering stress-strain curve) of epoxy nanocomposite adhesives has been studied. Two types of processing techniques such as conventional ultrasonic vibration (CUV) and ultrasonic dual mixing (UDM) were used to disperse nanoparticles in epoxy adhesive in order to develop epoxy nanocomposites. Aluminium-adhesive-aluminium joints were tested, and their fracture surfaces were characterized using FESEM to understand the role of toughening mechanisms on the performance of the joints. The outcome of the present study exhibited the importance of oxide nanoparticles in controlling the strength of epoxy adhesive based metal joints having significant applications in automobile and aerospace industry.

**KEYWORDS:** Epoxy adhesive; Nanoparticles; Processing technique; Lap shear performance.

#### Affiliation:

<sup>1</sup>Mads Clausen Institute, NanoSYD, University of Southern Denmark (SDU), Denmark

<sup>2</sup>Department of Applied Science, School of Engineering, University of Petroleum and Energy Studies, Dehradun-248007, Uttarakhand,

#### **Correspondence:**

goyatmanjeetsingh@gmail.com

#### 1. Introduction

Epoxide adhesives find extensive use in multiple industries, including automotive, aerospace, paint, coatings, and electrical [1-4]. Rigid oxide nanoparticles have garnered a lot of interest as fillers in recent years [5–7]. Because of their superior mechanical properties, chemical inertness, thermal stability at very high temperatures, and, of course, affordability when compared to other nanofillers like carbon

nanotubes [8-10], oxide nanoparticles like Al<sub>2</sub>O<sub>3</sub>, TiO<sub>2</sub>, and ZrO<sub>2</sub> [11–14] have been identified as potential candidates for the structural applications. Furthermore, compared to other nanofillers like carbon nanotubes, oxide nanoparticles' low aspect ratio ~ 1 provides less resistance to the polymer matrix's cross-linking density when incorporated into epoxy adhesives. However, because the van der Waals forces

This article is an open access article distributed under the terms and conditions of the Creative Commons Attribution (CC BY) license (https://creativecommons.org/licenses/by/4.0/).

become the greatest forces at the nanoscale in the range of 1–10 nm, the extremely high specific surface area of the nanoparticles enables them to attract each other due to attractive electrostatic van der Waals forces, leading in the development of agglomerates. To increase the various properties of the final nanocomposite material, it is extremely undesirable for the nanoparticles to agglomerate within the matrix [15]. Therefore, for the homogenous dispersion of nanoparticles in viscous epoxy, a particularly processing procedure is needed. effective nanoparticles added to epoxy adhesives have the potential to exacerbate the epoxy joints' primary weakness [16]. It was discovered that adding 2 wt% of Al<sub>2</sub>O<sub>3</sub> nanoparticles to epoxy adhesive significantly increases the adhesive's strength. When compared to neat epoxy adhesive, the Al<sub>2</sub>O<sub>3</sub>-epoxy nanocomposite adhesive exhibits a pull-off strength that is almost five times greater. According to the literature, the reason for the rise in adhesive joint qualities is a change in the joint's failure mode, which for neat epoxy exhibits interfacial failure and is changed to a mixed mode failure, such as partially cohesive and partially interfacial, for nanocomposite adhesive [16]. On the other hand, 5 w% of Al<sub>2</sub>O<sub>3</sub> nanoparticles added to an epoxy adhesive filmed on polyester random mat scrim causes a notable 15% increase in lap shear strength and 50% increase in peel strength for joints made of aluminium substrates [17]. According to certain research, the toughness and single lap shear strength of the joints are significantly increased when low content silica nanoparticles are added to a rubber toughened epoxy adhesive [18-20]. This rise can be attributed to various toughness mechanisms that have emerged, including fracture deflection and crack twisting around the nanoparticles, which have enhanced the plastic deformation of the epoxy matrix.

Over the years, various researchers studied the lap shear performance of epoxy nanocomposite adhesives consisting different size  $Al_2O_3$  and  $ZrO_2$  for various grades of Al and achieved some noticeable enhancement [17,21–23]. But most of the studies are incomplete and having limited information about the real cause of enhancement in the lap shear performance. Therefore, in the current study different types of oxide nanoparticles ( $TiO_2$ ,  $Al_2O_3$ , and  $ZrO_2$ ) and processing techniques are used to investigate the real cause of enhancement in lap joint performance of epoxy nanocomposite adhesives.

#### 2. Materials and methods

Two parts made up the epoxy adhesive (Loctite E60-HP): (i) epoxy resin (diglycidylether of bisphenol-A) and (ii) an amine-based hardener that was purchased as a base material from Loctite Hysol Company in the USA. Excellent bond strengths are offered by the high-performance epoxy to a broad range of metals and polymers. According to ASTM D-1002 and the technical data sheet, the typical lap shear strength of abraded aluminium is 29.92 MPa. Three different

types of oxide nanoparticles were obtained from American Elements Company in the USA:  $ZrO_2$  ( $\sim 25$  nm),  $TiO_2$  ( $\sim 48$  nm), and  $Al_2O_3$  ( $\sim 10$  nm). A 2.0 mm thick strip of extruded commercial aluminium (ASTM specification SB-209 Grade 1100) was utilized as the metal substrate in order to produce lap joints based on epoxy adhesive. The aluminium substrate was procured from an earlier tested source for its chemistry and mechanical properties [24].

https://www.rwpublisher.com/

## 2.1. Fabrication of epoxy nanocomposites

Two processing techniques were used to disperse oxide nanoparticles into the epoxy resin in order to produce nanocomposites. One is conventional ultrasonic vibration (CUV) [25,26] and the other is the ultrasonic dual mixing (UDM) [27,28].

## 2.2. CUV technique

The schematic diagram of CUV process is shown in **Fig. 1**. The optimized amount of TiO<sub>2</sub> nanoparticles (10 wt%) [26] was gradually added to the epoxy resin at ambient conditions and initially mixed via glass rod stirring for 5 min followed by addition of Methyl Ethyl Ketone (MEK) to the epoxy resin in a ratio of 4:1. The slurry (epoxy resin + nanoparticle + MEK) was further stirred for 5 min and then processed by the CUV process at optimized parameters described in detail in my earlier published work [26].

## 2.3. UDM technique

The schematic diagram of UDM route is shown in **Fig. 2**. The optimized amount of all nanoparticles such as  $TiO_2$  (10 wt%),  $Al_2O_3$  (3 wt%) and  $ZrO_2$  (5 wt%) were gradually added to the epoxy resin in separate beakers at ambient conditions and initially mixed via impeller stirring with a speed of 500 rpm for 5 min followed by addition of MEK to the epoxy resin in a ratio of 3:1. The slurry (epoxy resin + nanoparticle + MEK) was stirred for 5 min followed by UDM processing of it at optimized parameters described in detail in my earlier published work [27].

Using my previously reported method, the MEK was eliminated following CUV and UDM processing [27]. To ensure uniform mixing, the hardener was blended with the neat epoxy resin and nanoparticle containing epoxy resin in a stoichiometric weight ratio. The mixture was then agitated for 5 min at room temperature to release any trapped air. Afterwards, metal-epoxy-metal joints were created using degassed neat epoxy and epoxy nanocomposites.

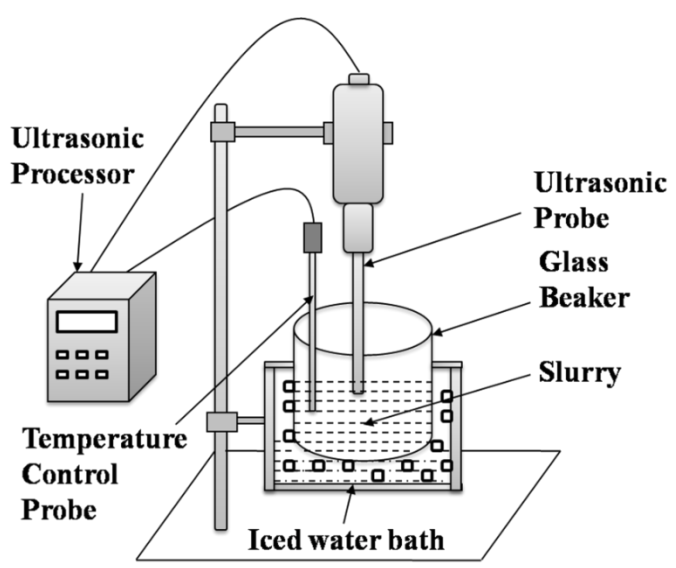


Fig. 1. The schematic diagram of CUV route.

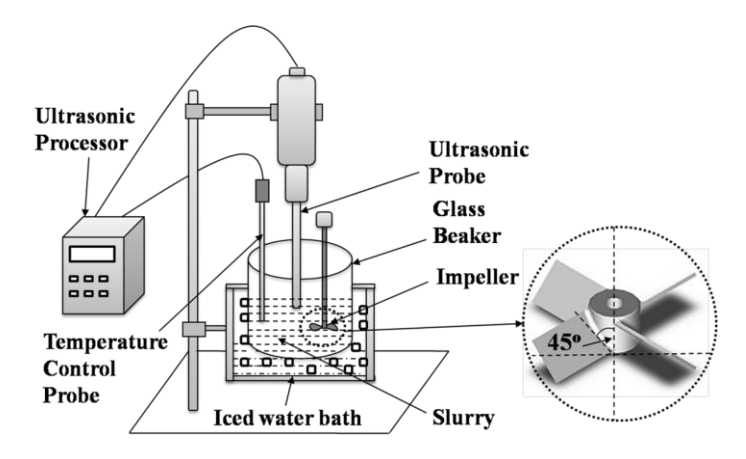


Fig. 2. The schematic diagram of UDM route.

### 2.4. Fabrication of lap shear joints

In order to prevent surface contamination caused by the existence of an excess oxide layer on the aluminium substrate, the surface of the substrate was mechanically polished using 400 grade emery paper [24] before the adhesive-based single lap joints were prepared. Acetone was used to clean the mechanically polished surface in order to get rid of any remaining grease or debris. On an aluminium substrate, the oxide nanoparticulate-epoxy composites and neat epoxy were placed progressively. Using a clamp tool, as seen in Fig. 3, a homogenous layer of adhesive measuring approximately ~ 0.1 mm was created. The clamp tool prevents the attached substrate from slipping while simultaneously maintaining a consistent bondline thickness. To minimize the impact of spit fillets, the extra adhesive was removed from the joint margins. Lastly, the single lap joints were allowed to cure at room temperature for a full day. ASTM-D1002 was followed in the preparation of neat epoxy adhesive and epoxy nanocomposite adhesives based single

lap shear joints of aluminium sheets. **Fig. 4** displays the dimensions of an adhesive-based single lap joint made of aluminium sheets in accordance with ASTM standards.

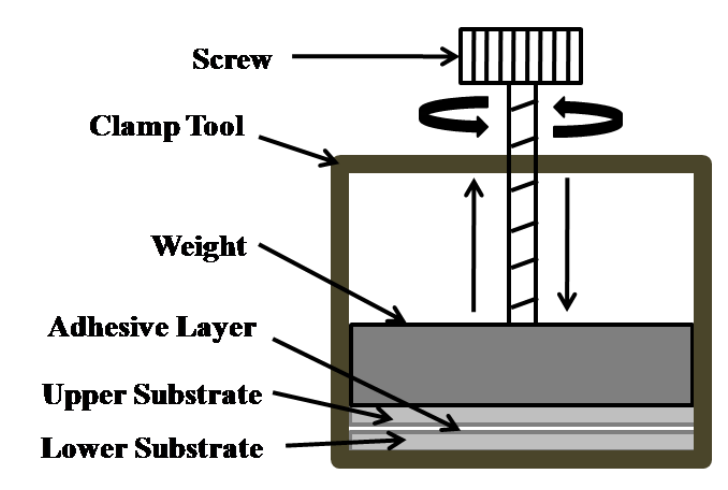


Fig. 3. Schematic diagram of clamp tool for single lap shear adhesive joint.

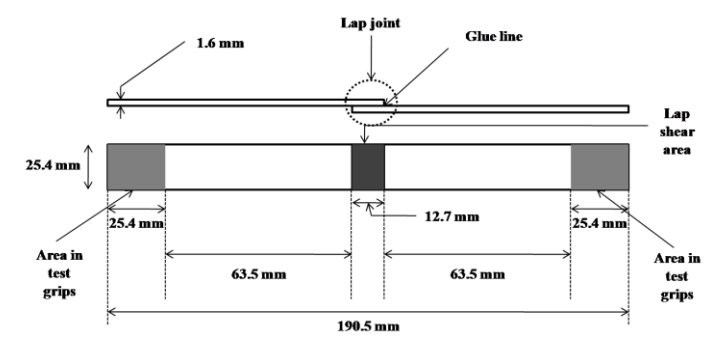


Fig. 4. Schematic diagram of Al-adhesive-Al based single lap joint.

#### 2.5. Characterizations

Lap shear joint test epoxy nanocomposites' surfaces, and the morphology of the aluminium substrate surface was examined using a field emission scanning electron microscope (FESEM). The acceleration voltage used to run FESEM (FEI, Quanta 200F) was 15 kV. A small layer of gold, approximately 6 nm in thickness, was plasma sprayed onto each specimen to facilitate electrical conduction and minimize surface charge during FESEM examination. Energy dispersive X-ray analysis (EDAX) was used to characterize the aluminium metal substrate. In order to determine the specimens' toughness and lap shear strength, tensile shear tests were performed in accordance with ASTM D1002 standard. A Universal Testing Machine (UTM) from Hounsfield (H25KS) conducted the testing under ambient conditions, with a crosshead speed of 1.3 mm/min. For each composition, the mean values with standard deviation of the three replicate specimens that underwent testing are presented.

#### 3. Results and Discussion

# 3.1. FESEM and EDAX analysis of Al substrate

The performance of any adhesive bonding primarily depends upon type of substrate material, preparation of surface of the substrate, wetting of the adhesive on the substrate, physical and chemical behavior of the adhesive and joint design [29]. The density and mechanical properties of the aluminum substrate such as elastic modulus, tensile strength and shear strength measured by standard tensile testing are found as 2.71g/cm<sup>3</sup>, 70-80 GPa, 110 MPa and 69 MPa respectively [24]. The FESEM images along with EDAX analysis of

aluminum substrate are shown in Fig. 5. The FESEM images (Fig. 5(a1, b1)) show the creation of uneven surface on the Al substrate due to abrasion which may increase the strength of the bonded joint by mechanical interlocking [24]. Furthermore, the creation of rough surface enhances the interfacial area of the joint and thus increases the interfacial surface tension of the substrate material prior to bonding [30]. The EDAX analysis of the relatively bright (Fig. 5(a1)) and grayish locations (Fig. 5(b1)) observed in the microstructure of Al substrate confirms the possibility of the presence of Al<sub>2</sub>O<sub>3</sub> and Al with some amount of Si as impurities (Fig. 5(a2, b2)). Generally, in case of the mechanically abraded Al substrates, the main bonding force primarily arises out of physical or mechanical interaction with the adhesive and thus more dependent on the contact area [31].

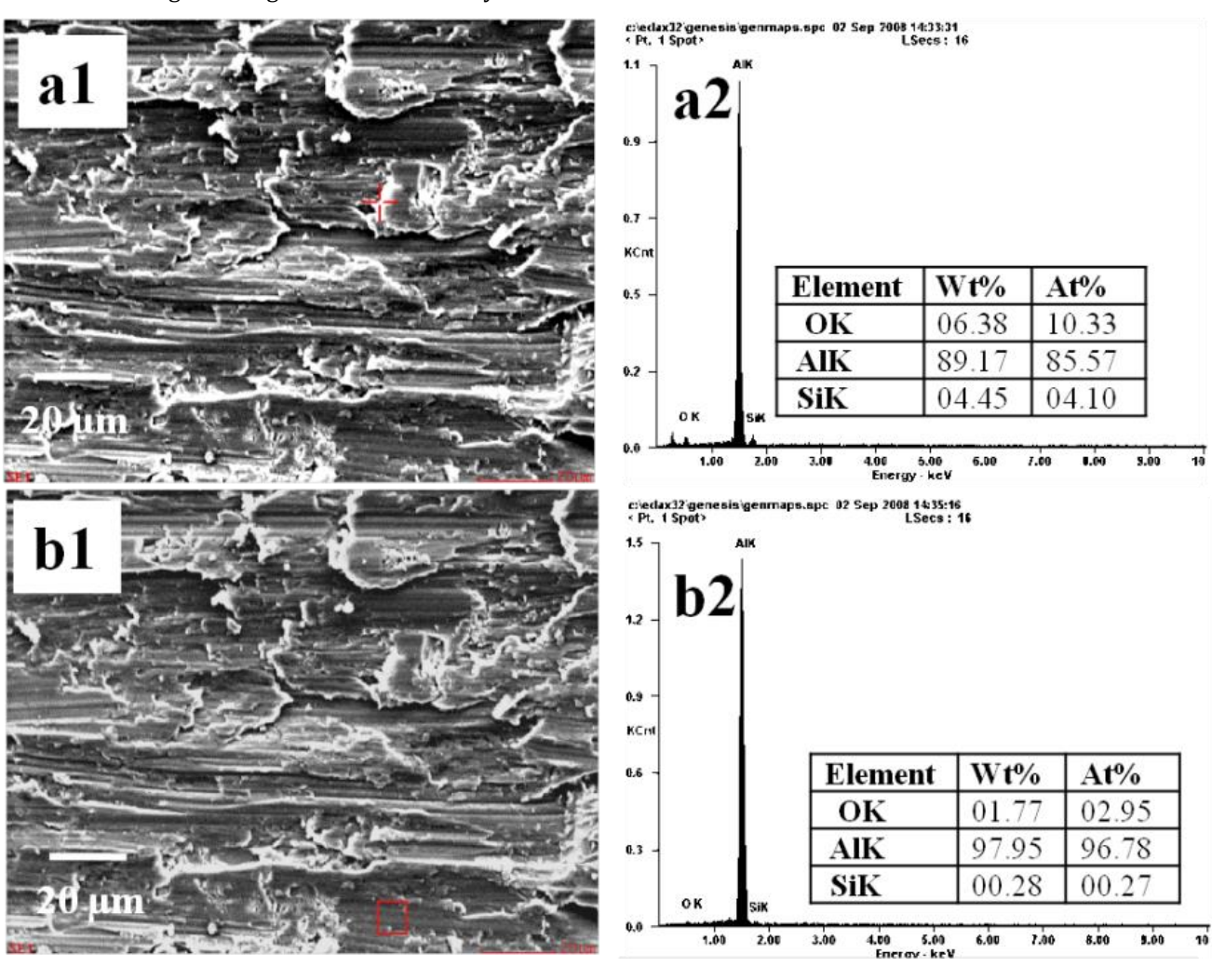


Fig. 5. FESEM images along with EDAX analysis of the Al substrate.

## 3.2. Lap shear strength analysis

**Fig. 6** displays the normal load-displacement curves from tensile shear tests of neat epoxy adhesive and epoxy nanocomposite adhesives. As might be predicted, the tidy

epoxy adhesive's load-displacement curve shows brittle failure. But epoxy nanocomposite adhesives' load-displacement curves also show brittle failure, albeit with more extension. This is explained by the fact that epoxy nanocomposites entail a number of failure and energy consumption processes [32]. Under some circumstances, the nanoparticles may cause matrix yielding. In addition, they act as stoppers to fracture growth by pinning them [33], which enhances the mechanical performance of epoxy nanocomposite adhesives.

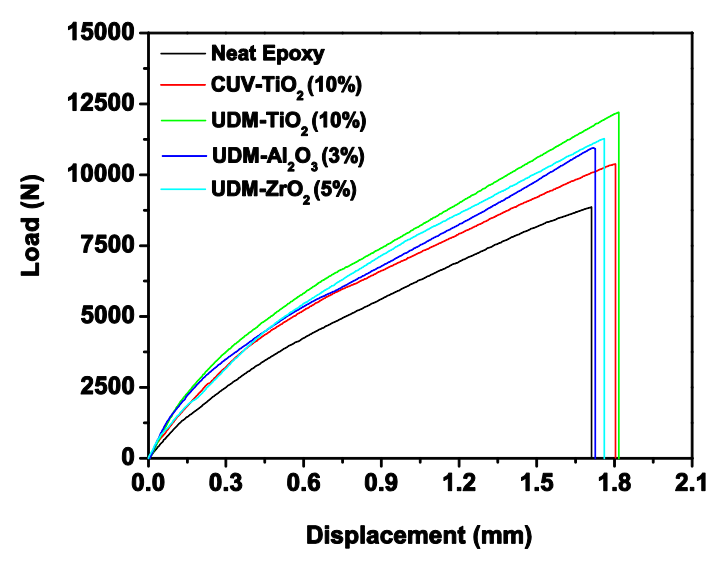


Fig. 6. Load-displacement curves of neat epoxy, CUV processed  $TiO_2$ -epoxy, UDM processed  $TiO_2$ -epoxy,  $Al_2O_3$ -epoxy and  $ZrO_2$ -epoxy nanocomposite adhesives.

The relative strength of adhesive-based joints was calculated by utilizing the following formula. Joint strength is calculated as follows:

$$Joint strenght = \frac{Failure load}{Adhesive lap area}$$
 (1)

Fig. 7 illustrates the lap shear joint strength of neat epoxy and epoxy nanocomposite adhesives. It is discovered that the neat epoxy adhesive has a lap shear strength of 27.5 MPa. It is evident that the lap shear strength is increased by the addition of oxide nanoparticles. When compared to pristine epoxy adhesive, the highest increase in lap shear strength for CUV processed TiO<sub>2</sub>-epoxy nanocomposite is approximately 17%, but for UDM processed TiO2-epoxy nanocomposite, it is approximately 38%. The noteworthy rise in the lap shear strength of the epoxy nanocomposite processed by UDM processing could potentially be attributed to UDM's superiority over CUV process when it comes to the dispersion of nearly single nanoparticles or their fine clusters inside the epoxy matrix [26,27]. Comparing the Al<sub>2</sub>O<sub>3</sub>-epoxy nanocomposite to the neat epoxy adhesive, the highest increase in lap shear strength is approximately 23%, whereas the ZrO<sub>2</sub>-epoxy nanocomposite exhibits a maximum increase of approximately 27%. The bond line thickness of the adhesive [24], as well as the surface treatment state of the metal substrate [34], are the primary determinants of the lap shear strength of an adhesive-based joint. These factors also have a substantial impact on the cohesive and adhesive strength of the joint. Because the oxide nanoparticulateepoxy composite adhesives' lap joint preparation processing parameters and the aluminium substrate's surface treatment are the same. Consequently, it is plausible to argue that the modification of the cohesive characteristics of the epoxy nanocomposites is the cause of the improvement in lap shear strength. The resistance to fracture provided by the nanoparticles that cause crack-blunting may be the main cause of the epoxy nanocomposite adhesive's increased joint strength [17].

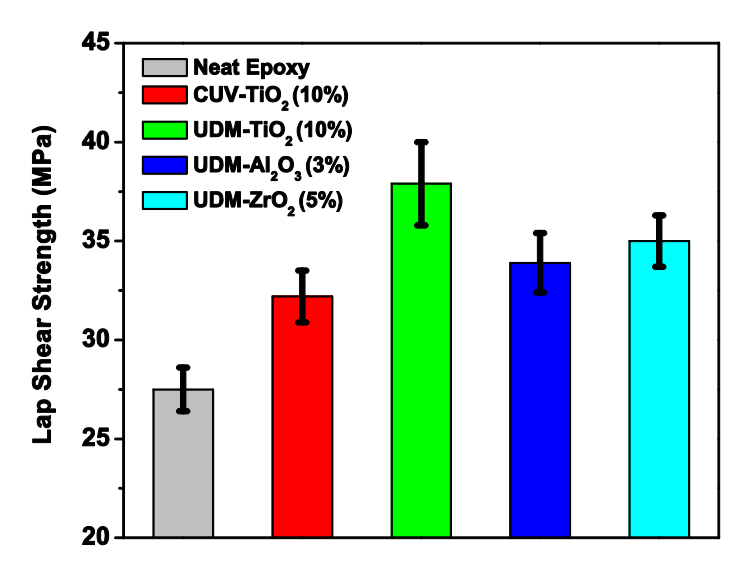


Fig. 7. Lap shear joint strength of neat epoxy, CUV processed  $TiO_2$ -epoxy, UDM processed  $TiO_2$ -epoxy,  $Al_2O_3$ -epoxy and  $ZrO_2$ -epoxy nanocomposite adhesives.

## 3.3. Lap shear joint toughness

The area under the stress-strain curve is used to determine the lap shear joint toughness of epoxy nanocomposites [35]. The load-displacement curves of the neat epoxy adhesive and epoxy nanocomposite adhesives were converted to stress-strain curves, which are displayed in **Fig. 8**, in order to calculate the area under the curves. **Fig. 9** displays the lap shear joint toughness of the nanocomposite adhesives ZrO2-epoxy, Al<sub>2</sub>O<sub>3</sub>-epoxy, CUV-processed TiO<sub>2</sub>-epoxy, and UDM-processed TiO<sub>2</sub>-epoxy. Because oxide nanoparticles are incorporated into the epoxy matrix, the epoxy nanocomposite adhesives have a substantially better lap shear joint durability than neat epoxy adhesives. When compared to neat epoxy adhesive, the highest increase in

joint toughness for a TiO<sub>2</sub>-epoxy nanocomposite produced by CUV is approximately 28%, but for a TiO<sub>2</sub>-epoxy nanocomposite processed by UDM, it is approximately 48%. The notable enhancement in the joint toughness of the TiO<sub>2</sub>-epoxy nanocomposite produced using UDM over CUV method could potentially be attributed to UDM's superiority in dispersing nearly individual nanoparticles or their fine clusters within the epoxy matrix [26,27]. Similarly, as compared to neat epoxy adhesive, the highest increase in joint toughness for Al<sub>2</sub>O<sub>3</sub>-epoxy nanocomposite is approximately 28%, but for ZrO<sub>2</sub>-epoxy nanocomposite adhesive, it is approximately 29%.

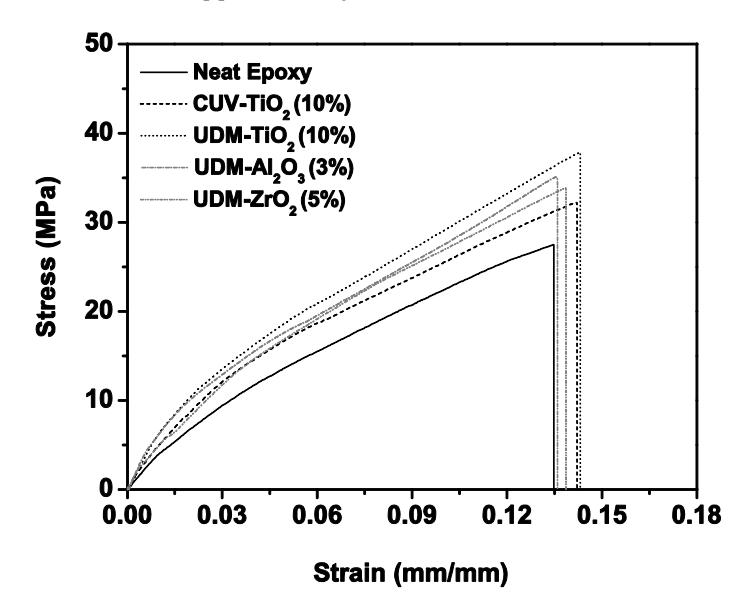
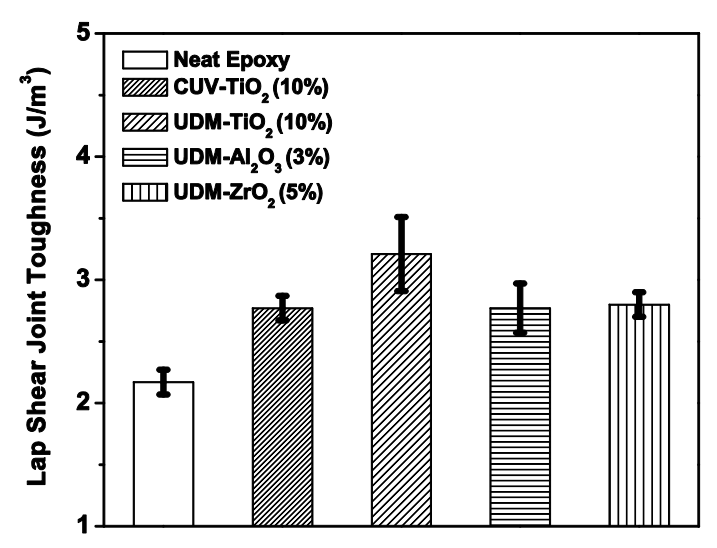


Fig. 8. Stress-strain curves of neat epoxy, CUV processed TiO₂-epoxy, UDM processed TiO₂-epoxy, Al₂O₃-epoxy and ZrO₂-epoxy nanocomposite adhesives.

The accumulated strain energy density that is released after failure is also known as the lap shear joint toughness, also referred to as the area under the stress-strain curve. An estimate of resistance to crack propagation and the energy absorbed during fracture can also be obtained from the strain energy density, which can be found from the area under the stress-strain curve. By absorbing stored strain energy and so slowing the crack propagation, the well-dispersed and closely spaced stiff nanoparticles can modify localized plastic shear yielding in the epoxy matrix and cause fracture diversion.



https://www.rwpublisher.com/

Fig. 9. Lap shear joint toughness of neat epoxy, CUV processed  $TiO_2$ -epoxy, UDM processed  $TiO_2$ -epoxy,  $Al_2O_3$ -epoxy and  $ZrO_2$ -epoxy nanocomposites adhesive.

# 3.4. Morphology of fracture surfaces of adhesive based joints

The fracture surfaces of CUV and UDM treated TiO<sub>2</sub>-epoxy nanocomposite adhesives, as well as neat epoxy adhesive are shown in **Fig. 10**. At the contact where the tidy epoxy adhesive and aluminium substrate meet (Fig. 10(a1)), the joint failed. However, in the case of the TiO2-epoxy nanocomposites produced by CUV and UDM, the joint failed partially at the adhesive-aluminium contact and partially cohesively within the adhesive; as a result, the characteristics differ, as shown by the neat epoxy FESEM images (Fig. **10(b1, c1)).** Similar to this, the joint failed partially at the interface and partially cohesively in the case of Al<sub>2</sub>O<sub>3</sub>-epoxy and ZrO<sub>2</sub>-epoxy nanocomposite adhesives produced by UDM (Fig. 11(a1, b1)). The high magnification FESEM images (Fig. 10(a2, a3)) show that the neat epoxy adhesive's fracture surface is extremely smooth, suggesting that if the stress reaches its critical value, the crack will spread quickly until the material fails. However, in contrast to the plain epoxy adhesive, the fracture surfaces of the CUV and UDM processed TiO<sub>2</sub>-epoxy nanocomposites (Fig. 10(b2, c2)), as well as the UDM processed Al<sub>2</sub>O<sub>3</sub>-epoxy and ZrO<sub>2</sub>-epoxy nanocomposites (Fig. 11(a2, b2)) look extremely rough. Additionally, as seen by the FESEM pictures, there was significant plastic deformation of the epoxy matrix in the case of the epoxy nanocomposite adhesives, which is indicative of fracture deflection and crack twisting around the nanoparticles [19].

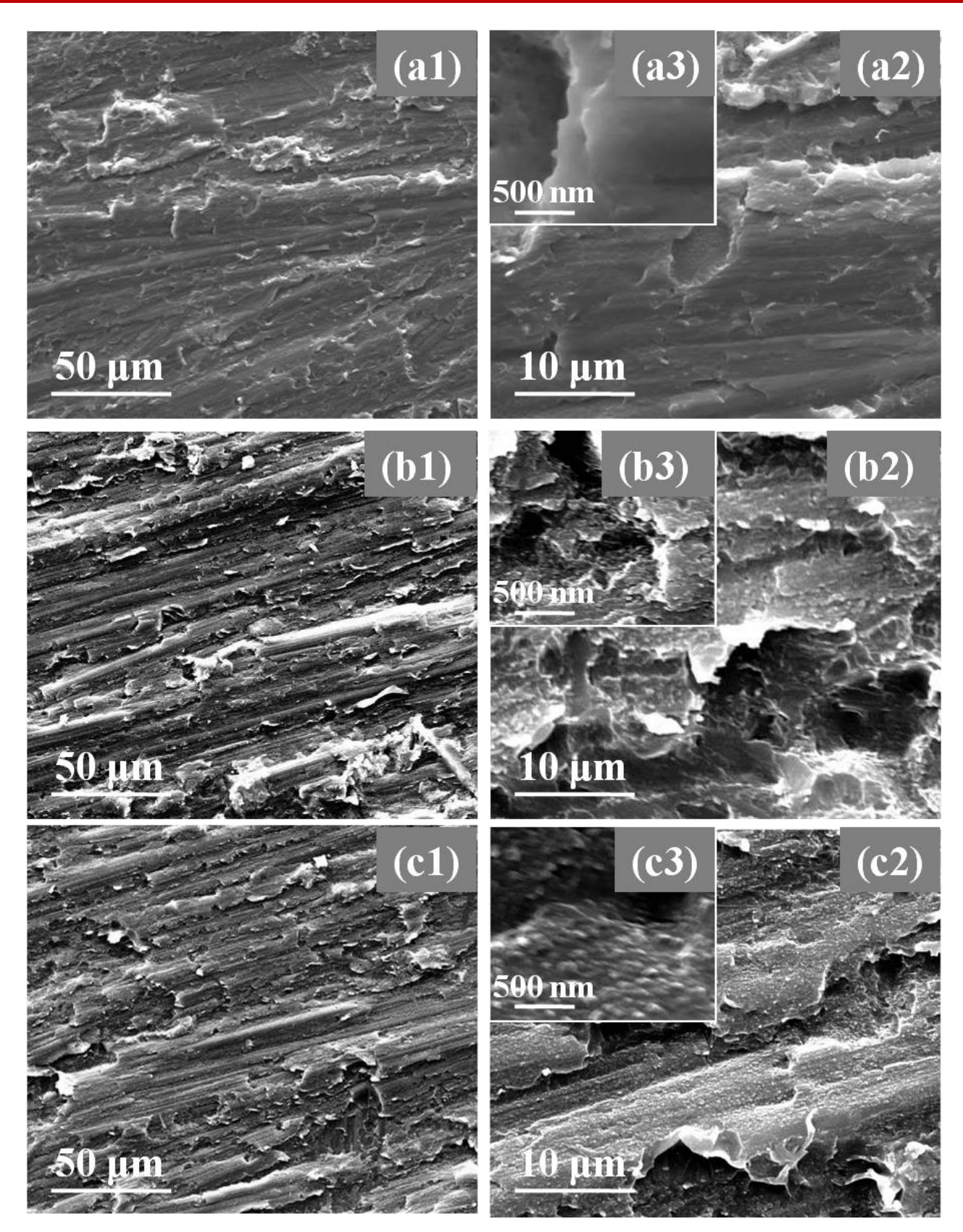


Fig. 10. FESEM images of lap shear joint fracture surfaces of (a) neat epoxy, (b) CUV and (c) UDM processed  $TiO_2$ -epoxy nanocomposites adhesive at different magnifications: (1) low, (2) high and (3) very high.

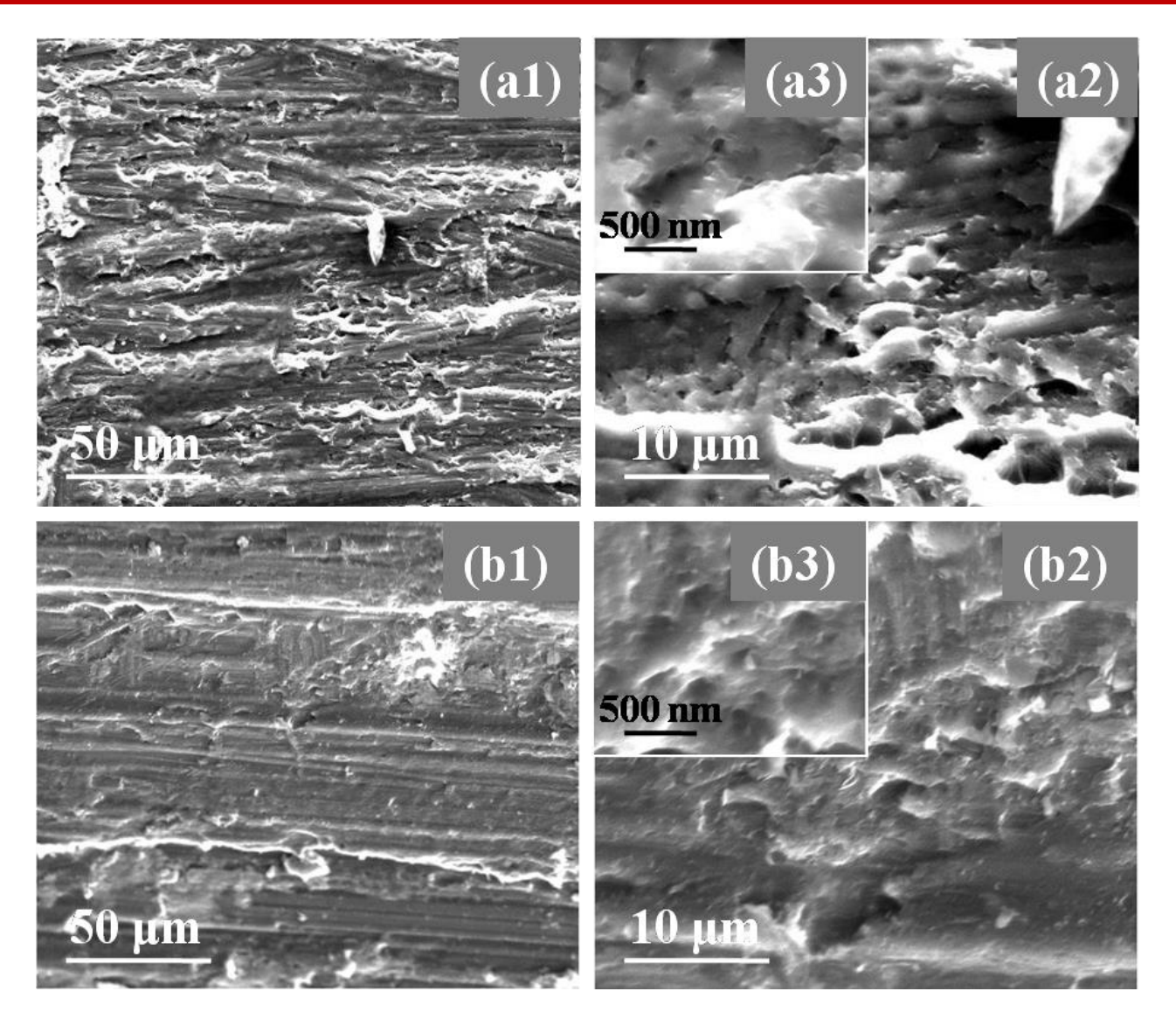


Fig. 11. FESEM images of lap shear joint fracture surfaces of (a) Al₂O₃-epoxy and (b) ZrO₂-epoxy nanocomposites adhesive at different magnifications: (1) low, (2) high and (3) very high.

Therefore, for aluminium joints bonded with epoxy nanocomposite adhesives, the change in joint failure mode from an interfacial failure for neat epoxy adhesive to a mixed mode of cohesive-interfacial failure is closely correlated with an increase in lap shear strength and lap joint toughness [21,36]. Because several toughening mechanisms, including crack deflection and crack twisting around the nanoparticles, are involved, the epoxy matrix's plastic deformation is enhanced, leading to an increase in joint toughness and lap shear strength [18,19]. Additionally, because of the mechanical anchoring mechanism, the nanoparticles can create new contact points and fill in the adherend's porosities, strengthening the interfacial strength. The enhanced adhesive strength of the nanocomposite adhesivebased joints is justified by the fact that epoxy nanocomposite adhesives also produce a higher wetting ability when compared to neat epoxy adhesive. The mechanical properties

of the epoxy matrix are significantly improved by the addition of oxide nanoparticles, albeit this enhancement is dependent on a number of variables, including the type of adhesive and adherend, the surface treatment used, and the property being tested [34]. They also rely on the kind and concentration of nanoparticles.

#### 4. Conclusions

The best concentration of TiO<sub>2</sub>, Al<sub>2</sub>O<sub>3</sub>, and ZrO<sub>2</sub> nanoparticles in epoxy nanocomposite adhesives improves the toughness and strength of the lap shear junction. The shift in the mechanism of joint failure from an interfacial failure for neat epoxy adhesive to a mixed mode cohesive-interfacial failure for nanoparticulate-epoxy composite adhesives is what accounts for the improvement in lap shear strength and lap joint toughness. According to FESEM pictures of epoxy

nanocomposite adhesives, the increased plastic deformation of the epoxy matrix is also responsible for the increase in lap shear strength and joint toughness. The superior ability of the UDM technique in regard to cluster breaking and homogenous distribution of nanoparticles in the epoxy matrix accounts for the notable improvement in the lap shear joint strength and joint toughness of the UDM processed TiO<sub>2</sub>-epoxy nanocomposite compared to the CUV processed TiO<sub>2</sub>-epoxy nanocomposite. This study demonstrated the significance of oxide nanoparticles in regulating epoxy adhesive strength, which has enormous potential in the automotive and aerospace industries.

#### Disclosure statement

The authors declare no relevant financial or non-financial interests.

### Data availability

Raw data of the research article is available with the authors and will be provided as per a request from the journal.

### Ethical approval

Not applicable.

#### References

- [1] A.K. Upadhyay, M.S. Goyat, A review on improved physical and thermal properties of oxide nanoparticles reinforced epoxy composites, Materials Protection 65 (2024). https://doi.org/10.62638/ZasMat1038.
- [2] A.K. Upadhyay, M.S. Goyat, A. Kumar, R. Nathawat, Taguchi design of experiments based optimization and experimental investigation of mechanical performance of hybrid epoxy nanocomposites, Materials Protection 64 (2023). https://doi.org/10.5937/zasmat2304433U.
- [3] R.R. Tummala, E.J. Rymaszewski, Y.C. Lee, Microelectronics Packaging Handbook, J Electron Packag 111 (1989) 241. https://doi.org/10.1115/1.3226540.
- [4] Q. Yao, J. Qu, Interfacial versus cohesive failure on polymer-metal interfaces in electronic packaging -Effects of interface roughness, Journal of Electronic Packaging, Transactions of the ASME 124 (2002) 127–134. https://doi.org/10.1115/1.1459470.
- [5] A. Aparna, A.S. Sethulekshmi, A. Saritha, K. Joseph, Recent advances in superhydrophobic epoxy based nanocomposite coatings and their applications, Prog Org Coat 166 (2022) 106819. https://doi.org/10.1016/j.porgcoat.2022.106819.

[6] A. Surendran, J. Pionteck, N. Kalarikkal, S. Thomas, Mechanical responses of epoxy/cloisite nanocomposites, Mater Chem Phys 281 (2022) 125755. https://doi.org/10.1016/j.matchemphys.2022.12575

https://www.rwpublisher.com/

- [7] M.S. Goyat, S. Sharma, S. Das, B.S. Tewari, M. Kumar, T.K. Gupta, C. Pant, Assessing thermo-mechanical and wetting properties of epoxy/SBA-15 nanocomposite, J Mater Sci 57 (2022). https://doi.org/10.1007/s10853-022-07769-6.
- [8] T.K. Gupta, S. Kumar, Fabrication of carbon nanotube/polymer nanocomposites, in: Carbon Nanotube-Reinforced Polymers: From Nanoscale to Macroscale, Elsevier Inc., 2018: pp. 61–81. https://doi.org/10.1016/B978-0-323-48221-9.00004-2.
- [9] B. Bittmann, F. Haupert, A.K. Schlarb, Preparation of TiO 2 epoxy nanocomposites by ultrasonic dispersion and resulting properties, J Appl Polym Sci 124 (2012) 1906–1911. https://doi.org/10.1002/app.34493.
- [10] P. Pötschke, A.R. Bhattacharyya, A. Janke, Carbon nanotube-filled polycarbonate composites produced by melt mixing and their use in blends with polyethylene, Carbon N Y 42 (2004) 965–969. https://doi.org/10.1016/j.carbon.2003.12.001.
- [11] T. Prasad, S. Halder, S.S. Dhar, M.S. Goyat, Epoxy/imidazole functionalized silica epoxy nanocomposites: Mechanical and fracture behaviour, Express Polym Lett 15 (2021). https://doi.org/10.3144/expresspolymlett.2021.19.
- [12] K. Kumar, M.S. Goyat, A. Solanki, A. Kumar, R. Kant, P.K. Ghosh, Improved mechanical performance and unique toughening mechanisms of UDM processed epoxy-SiO<inf>2</inf> nanocomposites, Polym Compos 42 (2021). https://doi.org/10.1002/pc.26280.
- [13] A. Marotta, N. Faggio, V. Ambrogi, A. Mija, G. Gentile, P. Cerruti, Biobased furan-based epoxy/TiO2 nanocomposites for the preparation of coatings with improved chemical resistance, Chemical Engineering Journal 406 (2021). https://doi.org/10.1016/j.cej.2020.127107.
- [14] M.S. Goyat, A. Hooda, T.K. Gupta, K. Kumar, S. Halder, P.K. Ghosh, B.S. Dehiya, Role of non-functionalized oxide nanoparticles on mechanical properties and toughening mechanisms of epoxy nanocomposites, Ceram Int 47 (2021). https://doi.org/10.1016/j.ceramint.2021.05.083.
- [15] F. Ali, M. Waseem, R. Khurshid, A. Afzal, TiO2 reinforced high-performance epoxy-co-polyamide composite coatings, Prog Org Coat 146 (2020) 105726. https://doi.org/10.1016/j.porgcoat.2020.105726.

- [16] L. Zhai, G. Ling, J. Li, Y. Wang, The effect of nanoparticles on the adhesion of epoxy adhesive, Mater Lett 60 (2006) 3031–3033. https://doi.org/10.1016/j.matlet.2006.02.038.
- [17] E.N. Gilbert, B.S. Hayes, J.C. Seferis, Nano-Alumina Modified Epoxy Based Film Adhesives, Polym Eng Sci 43 (2003) 1096–1104. https://doi.org/10.1002/pen.10093.
- [18] J.H. Klug, J.C. Seferis, Phase separation influence on the performance of CTBN-toughened epoxy adhesives, Polym Eng Sci 39 (1999) 1837–1848. https://doi.org/10.1002/pen.11577.
- [19] A.J. Kinloch, J.H. Lee, A.C. Taylor, S. Sprenger, C. Eger, D. Egan, Toughening structural adhesives via nanoand micro-phase inclusions, Journal of Adhesion 79 (2003) 867–873. https://doi.org/10.1080/00218460309551.
- [20] A.J. Kinloch, Toughening epoxy adhesives to meet today's challenges, MRS Bull 28 (2003) 445–448. https://doi.org/10.1557/mrs2003.126.
- [21] M. May, H.M. Wang, R. Akid, Effects of the addition of inorganic nanoparticles on the adhesive strength of a hybrid solgel epoxy system, Int J Adhes Adhes 30 (2010) 505–512. https://doi.org/10.1016/j.ijadhadh.2010.05.002.
- [22] A. Dorigato, A. Pegoretti, The role of alumina nanoparticles in epoxy adhesives, Journal of Nanoparticle Research 13 (2011) 2429–2441. https://doi.org/10.1007/s11051-010-0130-0.
- [23] A. Dorigato, A. Pegoretti, F. Bondioli, M. Messori, Improving epoxy adhesives with zirconia nanoparticles, Compos Interfaces 17 (2010) 873–892. https://doi.org/10.1163/092764410X539253.
- [24] P.K. Ghosh, S.K. Nukala, Characteristics of adhesive joints of metals using inorganic particulate composite adhesives, Transactions of the Indian Institute of Metals 61 (2008) 307–317. https://doi.org/10.1007/s12666-008-0044-z.
- [25] B. Bittmann, F. Haupert, A.K. Schlarb, Ultrasonic dispersion of inorganic nanoparticles in epoxy resin, Ultrason Sonochem 16 (2009) 622–628. https://doi.org/10.1016/j.ultsonch.2009.01.006.
- [26] M.S. Goyat, S. Rana, S. Halder, P.K. Ghosh, Facile fabrication of epoxy-TiO<inf>2</inf> nanocomposites: A critical analysis of TiO<inf>2</inf> impact on mechanical properties and toughening mechanisms, Ultrason Sonochem 40 (2018). https://doi.org/10.1016/j.ultsonch.2017.07.040.
- [27] M.S. Goyat, P.K. Ghosh, Impact of ultrasonic assisted triangular lattice like arranged dispersion of nanoparticles on physical and mechanical properties of epoxy-TiO2 nanocomposites, Ultrason Sonochem 42 (2018) 141–154. https://doi.org/10.1016/j.ultsonch.2017.11.019.

- [28] M.S. Goyat, S. Ray, P.K. Ghosh, Innovative application of ultrasonic mixing to produce homogeneously mixed nanoparticulate-epoxy composite of improved physical properties, Compos Part A Appl Sci Manuf 42 (2011). https://doi.org/10.1016/j.compositesa.2011.06.006.
- [29] A.N. Rider, D.R. Arnott, Boiling water and silane pretreatment of aluminum alloys for durable adhesive bonding, Int J Adhes Adhes 20 (2000) 209–220. https://doi.org/10.1016/S0143-7496(99)00046-9.
- [30] C. Spadaro, C. Dispenza, C. Sunseri, Influence of nanoporous structure on mechanical strength of aluminium and aluminium alloy adhesive structural joints, Journal of Physics Condensed Matter 18 (2006) S2007. https://doi.org/10.1088/0953-8984/18/33/S16.
- [31] S.G. Prolongo, G. Del Rosario, A. Ureña, Comparative study on the adhesive properties of different epoxy resins, Int J Adhes Adhes 26 (2006) 125–132. https://doi.org/10.1016/j.ijadhadh.2005.02.004.
- [32] C.H. Chen, J.Y. Jian, F.S. Yen, Preparation and characterization of epoxy/γ-aluminum oxide nanocomposites, Compos Part A Appl Sci Manuf 40 (2009) 463–468. https://doi.org/10.1016/j.compositesa.2009.01.010.
- [33] A.C. Roulin-Moloney, W.J. Cantwell, H.H. Kausch, Parameters determining the strength and toughness of particulate-filled epoxy resins, Polym Compos 8 (1987) 314–323. https://doi.org/10.1002/pc.750080506.
- [34] L.H. Phung, H. Kleinert, U. Füssel, L.M. Duc, U. Rammelt, W. Plieth, Influence of self-assembling adhesion promoter on the properties of the epoxy/aluminium interphase, Int J Adhes Adhes 25 (2005) 239–245. https://doi.org/10.1016/j.ijadhadh.2004.07.007.
- [35] M.Z. Rong, M.Q. Zhang, Y.X. Zheng, H.M. Zeng, K. Friedrich, Improvement of tensile properties of nano-SiO2/PP composites in relation to percolation mechanism, Polymer (Guildf) 42 (2001) 3301–3304. https://doi.org/10.1016/S0032-3861(00)00741-2.
- [36] S. Bhowmik, R. Benedictus, J.A. Poulis, H.W. Bonin, V.T. Bui, High-performance nanoadhesive bonding of titanium for aerospace and space applications, Int J Adhes Adhes 29 (2009) 259–267. https://doi.org/10.1016/j.ijadhadh.2008.07.002.